Indian J Phys
https://doi.org/10.1007/s12648-021-02228-5

ORIGINAL PAPER

Multiplicity per rapidity in Carruthers and hadron resonance gas approaches

A N Tawfik[1,2]*, M Hanafy[2,3] and W Scheinast[2,4]

[1]Nile University - Egyptian Center for Theoretical Physics (ECTP), Juhayna Square off 26th-July-Corridor, Giza 12588, Egypt

[2]World Laboratory for Cosmology And Particle Physics (WLCAPP), Cairo 11571, Egypt

[3]Physics Department, Faculty of Science, Benha University, Benha 13518, Egypt

[4]Joint Institute for Nuclear Research - Veksler and Baldin Laboratory of High Energy Physics, Moscow Region, Dubna, Russia 141980

Received: 09 April 2020 / Accepted: 16 October 2021

Abstract: The multiplicity per rapidity of the well-identified particles π^-, π^+, k^-, k^+, $\bar{p}$, p, and $p-\bar{p}$ measured in different high-energy experiments, at energies ranging from 6.3 to 5500 GeV, is successfully compared with the Cosmic Ray Monte Carlo event generator. For these rapidity distributions, we introduce a theoretical approach based on fluctuations and correlations (Carruthers approach) and another one based on statistical thermal assumptions (hadron resonance gas approach). Both approaches are fitted to both sets of results deduced from experiments and simulations. We found that the Carruthers approach reproduces well the full range of multiplicity per rapidity for all produced particles, at the various energies, while the HRG approach fairly describes the results within a narrower rapidity range. While the Carruthers approach seems to match well with the Gaussian normal distribution, ingredients such as flow and interactions should be first incorporated in the HRG approach. We conclude that fluctuations, correlations, interactions, and flow, especially in the final state, assure that the produced particles become isotropically distributed.

Keywords: Statistical theory and fluctuations; Relativistic heavy-ion collisions; Distribution theory and Monte Carlo studies

1. Introduction

Characterizing the particle production is seen as one of the main goals of the relativistic heavy-ion experiments [1]. By investigating the properties of the different produced particles throughout the various stages of the nuclear collision, essential information about partnoic such as quark glounplasma (QGP) and about hadronic phases can be obtained [2–7]. The various sophisticated nuclear processes starting from deconfined QGP and going through chiral and confinement phase transition(s) into confined hadrons, or vice versa—among others—are characterized by final stage particle production, i.e. fixed (chemically frozen) [8]. The information, which can be deduced from the different experiments such as the ones at the Super Protonsyncrotron (SPS) at CERN, the Relativistic Heavy Ion Collider (RHIC) at BNL, and the Large Hadron Collider (LHC) at CERN, on the characterization of the particle distributions and the dynamical evolution of such strongly interacting systems, for instance, elliptic and radial flow, manifests an essential property of the particle spectra [9]. Various quantities such as particle ratios, transverse mass spectra, and multiplicity per rapidity are also crucial in studying dynamics and different general properties, especially at the freezeout stage [10].

The rapidity distribution, for example, was studied in different approaches [11–28]. Assuming superposition of two fireballs along the rapidity axes, the Tsalis-type distribution was assumed to give a successful description for the rapidity distribution [12]. A thermodynamically consistent excluded volume model, in which flow is included, was proposed to nicely reproduce the rapidity distribution [9, 13]. A relative better description was obtained when longitudinal collective flow and excluded volume corrections have been taken into consideration [15, 16]. Impacts of the hydrodynamic flow have been introduced in refs.

*Corresponding author, E-mail: a.tawfik@cern.ch

Published online: 06 January 2022

[17, 18]. In a single statistical thermal freezeout model based on a single set of parameters, the rapidity distribution was fairly analyzed [21]. Also, in a hydrodynamical model with single particle spectra, the rapidity distribution was studied [22, 25]. The rapidity distribution was estimated in hydrodynamic models [23]. Extended statistical hadronization models have been utilized in describing the rapidity distribution [24]. In refs. [26, 27], an extended thermal model was used to calculate the particle spectra, at RHIC energies. The rapidity distribution was calculated assuming longitudinal hydrodynamic expansion of fluid created in the heavy-ion collisions [28]. The dependence of rapidity distribution on the transverse momentum was introduced in refs. [29–31].

In statistical models [26–28, 31–33], the chemical potential μ was successfully related to the rapidity y. Interested author on our almost entirely empirical estimation for chemical potential from measured transverse momentum distribution as function of rapidity is kindly advised to consult [29–31]. Accordingly, the rapidity distribution could be calculated over a wide large range of rapidity [31]. An extended longitudinal scalling was also introduced to the thermal model [33].

It is well known that the distributions of the various particles are not isotropic. Thus, it is obvious to conclude that the multiplicity per rapidity calculated within the hadron resonance gas (HRG) model should not convinsingly reproduce the experimental results, especially at a wide range of rapidity [13]. The inclusion of heavy resonances with their decay channels likely slightly improves the HRG reproduction of the measured rapidity multiplicities. The best HRG results are the ones within small-rapidity region. The present script presents other alternatives aiming at improving HRG [34–45]. This is the main motivation of the present script, namely improving various theoretical approaches towards a best description of the measured produced particles, at a wide range of energies. We also confront our results to the predictions gained from the Cosmic Ray Monte Carlo (CRMC) event generator [46–55], at energies ranging from 6.3 up to 5500 GeV. The CRMC event generator includes various hadronic interaction models such as EPOS1.99 and EPOSlhc models. In this context, we use EPOSlhc hadronic interaction model from high down to low energies.

For rapidity distributions measured in high-energy collisions and/or simulated in CRMC, we propose the utilization of Carruthers approach, which is based on hierarchy of cumulant correlation functions and their linked-pair approximation. This approach assumes an approximate translation invariance and utilizes a linking of averaged factorial moments to the second-order experimental moment in the final state of the particle production. For rapidity histograms, the various bins are assumed being irregular, i.e. they are influenced by fractal attractor or have an intermittent nature. The full range of rapidity $(\Delta y)^p$ can be then divided into smaller hypercubes of size $(\delta y)^p$, and thus, the ordinary bin-averaged factorial moments can be determined, which—in turn—can be expressed in a linked-pair approximation. Relating this to the negative binomial distribution makes it possible to propose a specific functional form such as Gaussian or a general exponential for the cumulants.

The aim of this work is to calculate the multiplicity per rapidity for various hadrons using the HRG model and Cosmic Ray Monte Carlo(CRMC) event generator[46–55] from low energies up to high energies. The CRMC event generator includes various hadronic interaction models such as EPOS1.99 and EPOSlhc models. In this context, we use EPOSlhc hadronic interaction model from high energies down to low energies. In the case of HRG model, we consider quantum statistics and boltzmann distribution. Also, another statistical method which is based on rapidity correlations from fluctuations of particle multiplicity is used. We compare our results with the available experimental data [34–36, 38–43]. The EPOSlhc results agree well with the experimental data for all considered particles but the HRG model with its two statistical methods cannot describe the experimental data in the full range of rapidity satisfactorily, but it can at midrapidity. In case of considering rapidity correlations from fluctuations of particle multiplicity, results can describe the experimental data successfully.

The present paper is organized as follows. We briefly introduce Carruthers and HRG approaches in Sect. 2. The results are discussed in Sect. 4. A detailed estimation of the multiplicity per rapidity is given in appendix A. The conclusions are outlined in Sect. 5.

2. Models

In this section, we give a brief description for the particle multiplicity as deduced from the HRG approach which is based on statistical thermal assumptions and the Carruthers approach which is based on correlations and fluctuations. The present work claims that these gradients seem to play an essential role in particle production.

2.1. HRG approach for rapidity multiplicity

It is widely known that the formation of resonances could be understood as bootstrap, i.e. the fireballs or resonances are demonstrated to be consisting of more smaller fireballs or lighter resonances, which—in turn—are composed of further smaller fireballs and lighter resonances, etc. For

such a system, the thermodynamics quantities can be derived directly from the partition function $Z(T,\mu,V)$, which in a Grand canonical ensemble reads [1]

$$Z(T,V,\mu) = \text{Tr}\left[\exp\left(\frac{\mu N - H}{T}\right)\right], \tag{1}$$

where H is Hamiltonian of the system, N is the total number of constituents, such as hadron resonances. In the HRG model, Eq. (1) can be expressed as a sum over all hadron resonances[1] The latter are coined as *missing states*.

$$\begin{aligned}\ln Z(T,V,\mu) &= \sum_i \ln Z_i(T,V,\mu) \\ &= \frac{Vg_i}{(2\pi)^3}\int_0^\infty \pm d^3p \,\ln\left[1 \pm \exp\left(\frac{\varepsilon_i(p)-\mu_i}{T}\right)\right],\end{aligned} \tag{2}$$

where $\pm$ stands for bosons and fermions, respectively, and $\varepsilon_i = \left(p^2 + m_i^2\right)^{1/2}$ is the dispersion relation of the ith particle, for which the total number of particles can be obtained as

$$N_i = T\frac{\partial Z_i(T,V)}{\partial \mu_i} = \frac{Vg_i}{(2\pi)^3}\int_0^\infty d^3p\left[\exp\left(\frac{\varepsilon_i(p)-\mu_i}{T}\right) \pm 1\right]^{-1}. \tag{3}$$

From Eq. (3), the invariant momentum spectrum of particles emitted from a thermal source can be derived [58, 59]

$$\frac{\mathrm{d}^3N_i}{\mathrm{d}y m_\mathrm{T}\mathrm{d}m_\mathrm{T}\mathrm{d}\phi} = \varepsilon_i\frac{Vg_i}{(2\pi)^3}\left[\exp\left(\frac{\varepsilon_i(p)-\mu_i}{T}\right) \pm 1\right]^{-1}, \tag{4}$$

where m_T is the transverse mass, which is given as $m_\mathrm{T} = \sqrt{m^2 + p_\mathrm{T}^2}$, where p_T is the transverse momentum. The energy of the ith particle, ε_i, can be then expressed in terms of the rapidity (y) and m_T as $\varepsilon = m_\mathrm{T}\cosh(y)$. Through integration over the full transverse mass m_T, the multiplicity N per rapidity y can be derived,

$$\begin{aligned}\frac{\mathrm{d}N}{\mathrm{d}y} = \sum_i \frac{Vg_i}{(2\pi)^2}\int_m^\infty \mathrm{d}m_\mathrm{T}\cosh(y)m_\mathrm{T}^2 \\ \left[\exp\left(\frac{m_\mathrm{T}\cosh(y)-\mu_i}{T}\right) \pm 1\right]^{-1}.\end{aligned} \tag{5}$$

Equation (5) can be rewritten as

$$\begin{aligned}\frac{\mathrm{d}N}{\mathrm{d}y} = \frac{g_i V}{2\pi^2}\left\{\frac{2T^3L_{i3}}{\cosh^2(y)}\left[\mp\exp\left(-\frac{m\cosh(y)-\mu_i}{T}\right)\right]\right. \\ \mp\frac{2mT^2}{\cosh(y)}L_{i2}\left[\mp\exp\left(-\frac{m\cosh(y)-\mu_i}{T}\right)\right]. \\ \left.\pm m^2T\log\left(1 \pm \left[\mp\exp\left(-\frac{m\cosh(y)-\mu_i}{T}\right)\right]\right)\right\}.\end{aligned} \tag{6}$$

where g_i is the degeneracy, and V is the volume of the fireball.

The freeze-out parameters; the baryon chemical potential (μ_i) and temperature (T), are then expressed in terms of the center-of-mass energy $\sqrt{S_{NN}}$ [1, 60]. The baryon chemical potential can be given as

$$\mu_B = \frac{a}{1 + b\sqrt{S_{NN}}}, \tag{7}$$

where $a = 1.245 \pm 0.094$ GeV, and $b = 0.264 \pm 0.028$ GeV^{-1}.

The temperature can be read as a function of the center-of-mass energy as [1, 60]

$$T = T_\mathrm{lim}\left[\frac{1}{1 + exp\left(\frac{1.172 - log(\sqrt{S_{NN}})}{0.45}\right)}\right]. \tag{8}$$

where $\sqrt{S_{NN}}$ is taken in GeV, and $T_\mathrm{lim} = 161 \pm 4$ MeV. The values of the freeze-out parameters are summarized in Table 1.

2.2. Carruthers approach for rapidity multiplicity

Suppose we have in the rapidity interval Δy, which is divided into X bins of length δy a histogram for rapidity y describing an event l. Consequently, the rapidity interval reads $\Delta y = X\delta y$. In the thermal models, the rapidity density of ith particle is given as two-particle correlation integral [61]

$$\frac{\mathrm{d}N^l(y)}{\mathrm{d}y} = \int_{\delta y}\rho'^l(y)\mathrm{d}y, \tag{9}$$

where $\rho'^l(y)$ is the probability density corresponding to the considered regions (*fireballs*) of the latest (final) hadron yields. This probability density $\rho'^l(y)$ can be expressed as [61]

$$\rho'^l(y) = \sum_\mathrm{i}\delta\left(y - y_\mathrm{i}^l\right), \tag{10}$$

in which $\delta\left(y - y_i^l\right)$ counts the available number of points y_i^l in the known interval δy for lth event, i.e. δ-function defines the rapidity bin width. For many events, the single particle density dN/dy related to the differential cross section $d\sigma/dy$ reads [61]

[1] either compiled by the particle data group [56] or still theoretical predictions [57].

Table 1 The freeze-out parameters as a function of the center-of-mass energy

$\sqrt{S_{NN}}$ (GeV)	μ (GeV)	T (GeV)
200	0.266 ± 0.005	0.152 ± 0.007
62.4	0.408 ± 0.006	0.126 ± 0.006
17.3	0.599 ± 0.009	0.088 ± 0.007
12.3	0.640 ± 0.006	0.073 ± 0.006
8.8	0.697 ± 0.004	0.060 ± 0.004
7.8	0.716 ± 0.008	0.054 ± 0.007
6.3	0.780 ± 0.006	0.048 ± 0.009

$$\frac{1}{\sigma_{\mathrm{i}}}\frac{\mathrm{d}\sigma}{\mathrm{dy}}=\frac{1}{N^{l}}\sum_{\mathrm{i}}\frac{\mathrm{d}N^{l}}{\mathrm{dy}} \tag{11}$$

where N^l is the total number of particles and σ_i is the corresponding cross section. This can be converted into a statistical ensemble having a probability density $\rho(y_1, y_2, \ldots, y_N)$ for the distributed points y_{i}, where $i = 1, 2, \ldots, N$ stand for particles within th interval Δy. Thus, Eq. (11) can be rewritten as [61]

$$\begin{aligned}
&\frac{1}{\sigma_i}\frac{\mathrm{d}\sigma}{\mathrm{dy}}\equiv\rho_1(y)=\left\langle\sum_{\mathrm{i}}\delta(y-y_{\mathrm{i}})\right\rangle,\\
&\frac{1}{\sigma_{\mathrm{i}}}\frac{\mathrm{d}^2\sigma}{\mathrm{dy_1dy_2}}\equiv\rho_2(y_1,y_2)=\left\langle{\sum_{\mathrm{i,j}}}'\delta(y_1-y_{\mathrm{i}})\delta\big(y_2-y_{\mathrm{j}}\big)\right\rangle,\\
&\frac{1}{\sigma_i}\frac{\mathrm{d}^3\sigma}{\mathrm{dy_1dy_2dy_3}}\equiv\rho_3(y_1,y_2,y_3)\\
&\qquad=\left\langle{\sum_{i,j,k}}'\delta(y_1-y_{\mathrm{i}})\delta\big(y_2-y_{\mathrm{j}}\big)(y_3-y_{\mathrm{k}})\right\rangle,
\end{aligned} \tag{12}$$

where ρ_q is the rapidity distribution of correlation functions and the hat to the summation refers to exclusion of terms with equal indices. Equation (12) enables simplified calculations for the integrating the correlations from the fluctuations of the particle multiplicity considering different domains in the rapidity ranges. Assuming a domain Q_2 with equal ranges Δy of y_i, thus Eq. (9) can be expressed as follows [62].

$$\begin{aligned}
&\int_{Q_1}\rho_1(y_1)\mathrm{dy}_1=\langle N\rangle_{Q_1},\\
&\int_{Q_2}\rho_2(y_1,y_2)\mathrm{dy}_1\mathrm{dy}_2=\langle n(n-1)\rangle_{Q_2},\\
&\int_{Q_3}\rho_3(y_1,y_2,y_3)\mathrm{dy}_1\mathrm{dy}_2\mathrm{dy}_3=\langle n(n-1)(n-2)\rangle_{Q_3}.
\end{aligned} \tag{13}$$

For application in high-energy analysis, the factorial moments of the averaged bin for $\rho = 2$ can be rewritten as [61]

$$\int_{Q_2}\rho_2(y_1,y_2)\mathrm{dy}_1\mathrm{dy}_2=\sum_{k=1}^{X}\langle n_k(n_k-1)\rangle, \tag{14}$$

where n_k is the number of particles in bin (k). The summation over hypercubes in higher dimensions $Q_q = \sum(\delta y)^n$ gives (a generalization to Q_q):

$$\begin{aligned}
&\int_{Q_q}\rho_q\big(y_1,y_2,\ldots,y_q\big)\mathrm{dy}_1\mathrm{dy}_2\ldots\mathrm{dy}_q\\
&\quad=\sum_{k=1}^{X}\langle n_k(n_k-1\ldots(n_k-n-1))\rangle.
\end{aligned} \tag{15}$$

When removing the symmetry of low-order density correlations, the cumulants can be used. The correlation functions of the cumulants $\big(c_p\big)$ can then be expressed in terms of correlation densities and vice versa as follows (number of permutations in the sums are shown in brackets) [62].

$$\begin{aligned}
\rho_2(1,2)&=\rho_1(1)\rho_1(2)+c_2(1,2),\\
\rho_3(1,2,3)&=\rho_1(1)\rho_1(2)\rho_1(3)\\
&\quad+\sum_{(3)}c_2(1,2)\rho_1(3)+c_3(1,2,3),\\
\rho_4(1,2,3,4)&=\rho_1(1)\rho_1(2)\rho_1(3)\rho_1(4)\\
&\quad+\sum_{(4)}\rho_1(1)\rho_1(2)c_2(3,4)\\
&\quad+\sum_{(3)}c_2(1,2)c_2(3,4)+\sum_{(4)}c_3(1,2,3)\rho_1(4)\\
&\quad+c_4(1,2,3,4).
\end{aligned} \tag{16}$$

The factorial of cumulant moments $\big(f_q\big)$ reads [61]

$$f_2=\langle n(n-1)\rangle-\langle n\rangle^2, \tag{17}$$

$$f_3=\langle n(n-1)(n-2)\rangle-3\langle n(n-1)\rangle\langle n\rangle+2\langle n\rangle^3, \tag{18}$$

and so on, are just integrals of the corresponding cumulants $\big(c_p\big)$.

The moments can then be averaged over all bins, $\big[\bar{n}=\bar{\rho}\delta y=\sum_{m=1}^{X}\langle n_m\rangle/X\big]$ or to the local average $\langle n_m\rangle\equiv\bar{\rho_m}\delta y$, where X are numbers of identical widths (δy) normalized either to the overall mean number per bin. These choices are usually referred to as "horizontal" and "vertical" averages, respectively, [61]

$$F_q^h\equiv\frac{1}{X(\delta y)^q}\sum_{m=1}^{X}\int_{Q_m}\prod_i\mathrm{dy}_i\frac{\rho_q\big(y_1\ldots y_q\big)}{\bar{\rho^q}}, \tag{19}$$

$$F_q^v \equiv \frac{1}{X}\sum_{m=1}^{X}\frac{\langle n_m(n_m-1)\ldots(n_m-q+1)\rangle}{\langle n_m\rangle^q}. \tag{20}$$

Recalling the factorial cumulants of the averaged bin

$$\begin{aligned} K_q^h(\delta y) &\equiv \frac{1}{X}\sum_{m=1}^{X}\frac{f_q^m}{\bar{n^q}} \\ &= \sum_m \frac{N_m(N_m-1)}{2\sqrt{\pi}\sigma_{\mathrm{T}}} e^{-y^2/4\sigma_{\mathrm{T}}^2}, \end{aligned} \tag{21}$$

$$\begin{aligned} K_q^v(\delta y) &\equiv \frac{1}{X}\sum_{m=1}^{X}\frac{f_q^m}{\langle n_m\rangle} \\ &= \frac{1}{X(\delta y)^q}\sum_{m=1}^{X}\int_{Q_m}\prod_i \mathrm{d}y_i \frac{c_q(y_1\ldots y_q)}{\langle\bar{\rho_m}\rangle^q} \\ &= \sum_{m\neq m'}\frac{N_m N_{m'}}{2\sqrt{\pi}\sigma_{\mathrm{T}}} e^{-(y-\bar{y}_m+\bar{y}_{m'})^2/4\sigma_{\mathrm{T}}^2}. \end{aligned} \tag{22}$$

It is obvious that when the values of one variable, such as (y_1), approach zero, the dependence on y_2 of the correlated particle could be fitted as an either exponential or Gaussian distribution in order to deduce the cumulant K_2 [61]

$$K_2 \equiv \frac{\rho_2(y_1,y_2)-\rho_1(y_1)\rho_1(y_2)}{\rho_1(y_1)\rho_1(y_2)} \approx \gamma_2 e^{-(y_1-y_2)^2/4\lambda^2}, \tag{23}$$

where the rapidity density of a source n emitting $\int dy\rho_1^{(m)}(y)$ particles is to be determined as [63]

$$\rho_1^{(n)} \approx \sum_{\mathrm{n}}\frac{N_{\mathrm{n}}}{\sqrt{2\pi}\sigma_{\mathrm{T}}} e^{-\frac{1}{2}(y-\bar{y}_{\mathrm{n}})^2/\sigma_{\mathrm{T}}^2}, \tag{24}$$

and then can be related to dN/dy, directly.

3. Cosmic Ray Monte Carlo (CRMC) model

As introduced, the hybrid Cosmic Ray Monte Carlo (CRMC EPOSlhc) event generator shall be utilized in generating various multiplicity per rapidity for different hadrons, at energies ranging between $\sqrt{s_{NN}} = 6.3$ and 5500 GeV. The CRMC EPOSlhc results are then compared with the available experimental data and finally fitted by the HRG and Carruthers approaches.

The CRMC is an interface for the various cosmic ray Monte Carlo models for various effective quantum chromodynamic (QCD) models and different experiments such as CMS, ATLAS, LHCb, NA61 and the ultra high-energy cosmic rays observatory Pierre Auger. It includes different types of interactions that are built on the highly Gribov-Regge model-like EPOSlhc/1.99. CRMC introduces a full description for background taking into consideration the resultant diffraction. Its interface can access the resultant output from various event generators for heavy-ion collisions. CRMC interface is also connected to a wide spectrum of models, such as qgsjet01 [46, 47], qgsjetII [48–50], sibyll [51–53] and EPOS 1.99/lhc [54, 55]. QGSJET01 and SIBYLL2.3, at low energies, EPOS lhc/1.99, QGSJETII v03 and v04 are the interaction models that can be integrated at high energies.

In the present paper, we utilize the CRMC EPOSlhc event generator which has various parameters for the primordial observables in high-energy collisions and their phenomenological assumptions. These can be modified due to theoretical and experimental postulates. It was argued that EPOSlhc is able to give a reasonable description for heavy-ion collisions regarding the generated data from various experiments and also other event generators [54, 55].

EPOSlhc was originally constructed for cosmic ray air showers and could be utilized for pp- and AA-collisions, at SPS, RHIC, and LHC energies. EPOSlhc even uses a more simplified treatments for heavy-ion collisions at the last stage of their evolutions and thus can be applied for minimum bias in the interactions between hadrons in the nuclear collisions [64]. EPOSlhc is a parton model with various parton–parton interactions resulting in various parton ladders and provides a good estimation for particle yields, multiple scattering of partons, evaluations of cross section, shadowing and screening through splitting and unitarization, and various collective effects of hot and dense media. It should be mentioned that EPOSlhc does not consider the simulations for complete hydrosystem even in the last stage.

In the present work, we utilize EPOSlhc event generator, at energies spanning between 6.3 and 5500 GeV for an ensemble of at least 100, 000 events per energy. We have calculated the multiplicity for π^-, π^+, k^-, k^+, $\bar{p}$, p, and $p-\bar{p}$ in various rapidity windows $-6<y<6$. Proving the validity of the hybrid EPOSlhc event generator, we hope at calculating the multiplicity per rapidity for the considered various hadrons, which is assumed to come up with a novel input for the future facilities NICA and FAIR, for instance.

4. Results and discussion

The present analysis is based on a reproduction of experiments results for the multiplicity per rapidity dN/dy of π^-, π^+, k^-, k^+, $\bar{p}$, p, and $p-\bar{p}$ [34–36, 38–43], at energies ranging between 6.3 and 5500 GeV. We also compare with results deduced from EPOSlhc event generator [54, 55]. Both sets of results are then confronted to the HRG thermal

and the Carruthers rapidity approaches, in which the dependence of the freezeout temperature T and the baryon-chemical potential μ_B on the center-of-mass energy $\sqrt{s_{NN}}$ is shown in Table 1.

The present work aims at updating the study of the multiplicity per rapidity in the HRG model. One of the improvements we are presenting here is the inclusion of various missing states to the well-known hadron states recently reported by the particle data group [56]. The missing states are hadron resonances which are theoretically predicted [57], but not yet confirmed, experimentally. Their physical characteristics including masses and other quantum numbers, etc., are theoretically well known. It was conjectured that these states greatly contribute to the fluctuations and the correlations simulated in the recent lattice QCD calculations [65]. Best reproduction of fluctuations and the correlations are among the main motivations to add these hadron states to the HRG model [66]. Regardless the corresponding limitations, we intend to check whether the new hadron states contribute to the multiplicity per rapidity of π^-, π^+, k^-, k^+, $\bar{p}$, p, and $p-\bar{p}$, as the missing states likely come up with additional degrees of freedom and certainly considerable decay channels which might affect the final number of particles produced.

Also, the present work introduces a new approach based on Carruthers proposal for hierarchy of cumulant correlation functions and their linked-pair approximation, which satisfactorily characterizes the galaxy correlation and successfully describes the central rapidity domain [61]. The basic idea is an approximate translation invariance and a linking of averaged factorial moments to the second-order experimental moment in the final state of the particle production. As for rapidity histograms, it was assumed that the various bins are likely irregular, i.e. they are influenced by fractal attractor, e.g. intermittence, where the full range of rapidity $(\Delta y)^p$ is divided into smaller hypercubes of size $(\delta y)^p$. An ordinary bin-averaged factorial moments can be determined, which can then be expressed in linked-pair approximation. This—in turn—can be related to the negative binomial distribution. For the high-energy collisions, a specific functional form such as Gaussian or an exponential can be proposed for the cumulants or the correlation functions, Eq. (24).

The results obtained are compared with both experiment and event generator. For almost all particles, the dependence of the multiplicity per rapidity dN/dy on the rapidity y was fitted to Gaussian normal distribution function,

$$\frac{\mathrm{d}N}{\mathrm{d}y} = a_0 \exp\left\{-0.5\left[\left(\frac{y-a_1}{a_2}\right)\left(\frac{y-a_1}{a_2}\right)\right]\right\}, \tag{25}$$

where a_0, a_1, and a_2 are the fit parameters, Table 2. Particularly for net proton $p-\bar{p}$, we use the binomial

$$\frac{\mathrm{d}N}{\mathrm{d}y} = c_0 + c_1 y + c_2 y^2 + c_3 y^3, \tag{26}$$

in which c_0, c_1, c_2, and c_3 are free parameters, Table 3.

Figure 1 shows the multiplicity per rapidity dN/dy versus y in a semi-log scale. The experimental results for π^-, π^+, k^-, k^+, $\bar{p}$, p, and $p-\bar{p}$ [34–36, 38–43] (symbols) are compared with the CRMC EPOSlhc event generator [54, 55] (dashed curves). At the Large Hadron Collider (LHC) energies, 2760 and 5500 GeV, we introduce CRMC predictions. To the authors best knowledge, such measurements are not yet available to depict and compare with. The experimental results available are fitted to the hadron resonance gas (HRG) approach (dash-dotted curves), Eq. (6) or Eq. (25) and to the Gaussian distribution function (solid curve). For a better comparison, we keep the same dN/dy- and y-scales in all panels devoted to the different particle yields.

There is a general observation that for all particles when the energy decreases, especially from top RHIC down to low SPS, i.e. from 200 down to 6.3 GeV, when disregarding our CRMC-predictions at LHC energies, the statistical fits seem becoming better and better. $\bar{p}$ and $p-\bar{p}$ are exceptions. Their fits become worse with decreasing the energy. Also, we generally observe that the HRG model can excellently describe both experimental and simulation results up to a relative narrow range around mid-rapidity. For a wider y-range, the ability of the HRG model to reproduce the results deduced from the experiments and the simulations becomes more and more worse. These are generic observations, from which final conclusions can be drawn. The goodness of the statistical fits shall be estimated, quantitatively. We find that the results from the CRMC EPOSlhc event generator match well with the experimental results. Accordingly, we present predictions, at LHC energies. Also, we observe that dN/dy for the net-proton $p-\bar{p}$ seems to have two peaks. This might be understood due to the binomial assumed for this particle yield. For π^-, π^+, k^-, k^+, $\bar{p}$, and p, the fit parameters V and m, i.e. the volume of the fireball and the mass of the particle, respectively, are listed in Table 2. For net-proton $p-\bar{p}$, the corresponding fit parameters as deduced from Eq. (26) are given in Table 3.

Figure 2 shows dN/dy versus y from Caruthers rapidity approach, Eq. (24), and CRMC EPOSlhc event generator compared with the experimental data [34–36, 38–43]. We conclude that the results on dN/dy excellently agree well with the CRMC EPOSlhc event generator. The agreement with CRMC is also excellent. The goodness of corresponding fits is outlined in Table 2.

In light of this, we conclude that the correlations and fluctuations of the particle multiplicity as included in the Carruthers approach are essential for a better reproduction

Table 2 The fit parameters obtained from the HRG approach for rapidity distributions for π^-, π^+, k^-, k^+, $\bar{p}$ and p, at various energies

Particle	$\sqrt{S_{NN}}$ (GeV)	a_0	a_1	a_2	χ^2/dof	V	m (GeV)
π^-	200	308.369 ± 0.584	$-4.752 \times 10^{-3} \pm 5.107 \times 10^{-3}$	$2.341 \pm 5.661 \times 10^{-3}$	0.888	$5.536 \times 10^5 \pm 1.897 \times 10^4$	0.127 ± 0.099
	62.4	226.487 ± 4.722	$1.711 \times 10^{-3} \pm 7.783 \times 10^{-2}$	$1.778 \pm 6.893 \times 10^{-2}$	120.8	$4.938 \times 10^5 \pm 6.482 \times 10^4$	0.082 ± 0.087
	17.3	180.989 ± 0.581	$-6.108 \times 10^{-6} \pm 5.299 \times 10^{-3}$	$1.436 \pm 5.371 \times 10^{-3}$	0.568	$6.392 \times 10^5 \pm 5.243 \times 10^4$	0.062 ± 0.032
	12.3	148.9 ± 0.598	$-1.595 \times 10^{-3} \pm 5.926 \times 10^{-3}$	$1.279pm6.479 \times 10^{-3}$	0.518	$3.674 \times 10^5 \pm 4.874 \times 10^4$	0.077 ± 0.016
	8.8	115.246 ± 0.999	$4.526 \times 10^{-4} \pm 1.136 \times 10^{-2}$	$1.135 \pm 1.152 \times 10^{-2}$	1.342	$3.261 \times 10^5 \pm 5.025 \times 10^4$	0.055 ± 0.012
	7.8	104.838 ± 1.835	$8.039 \times 10^{-3} \pm 2.104 \times 10^{-2}$	$1.045 \pm 2.086 \times 10^{-2}$	4.144	$6.231 \times 10^5 \pm 4.639 \times 10^4$	0.025 ± 0.0067
	6.3	88.074 ± 0.272	$4.068 \times 10^{-3} \pm 3.567 \times 10^{-3}$	$1.004 \pm 3.554 \times 10^{-3}$	0.086	$2.785 \times 10^5 \pm 4.062 \times 10^4$	0.0076 ± 0.009
π^+	200	298.692 ± 1.479	$-2.327 \times 10^{-4} \pm 1.348 \times 10^{-2}$	$2.265 \pm 1.445 \times 10^{-2}$	17.22	$5.481 \times 10^5 \pm 6.932 \times 10^4$	0.132 ± 0.081
	62.4	-490.308 ± 0.025	-0.051 ± 0.03	1.826 ± 2.588	31.15	$5.086 \times 10^5 \pm 6.602 \times 10^4$	0.074 ± 0.052
	17.3	159.21 ± 1.932	$2.579 \times 10^{-3} \pm 2.28 \times 10^{-2}$	$1.548 \pm 2.499 \times 10^{-2}$	27.441	$5.021 \times 10^5 \pm 1.821 \times 10^4$	0.056 ± 0.067
κ^-	200	907.015 ± 12.609	$3.379 \times 10^{-3} \pm 0.033$	$2.066 \pm 3.294 \times 10^{-2}$	34.44	$3.843 \times 10^5 \pm 5.321 \times 10^4$	0.231 ± 0.0421
	62.4	358.495 ± 8.401	$2.049 \times 10^{-3} \pm 4.630 \times 10^{-2}$	$1.570 \pm 3.731 \times 10^{-2}$	12.304	$2.653 \times 10^5 \pm 4.520 \times 10^4$	0.045 ± 0.0088
	17.3	17.505 ± 0.353	$1.311 \times 10^{-3} \pm 1.95 \times 10^{-2}$	$1.0673 \pm 2.692 \times 10^{-2}$	0.472	$4.872 \times 10^5 \pm 5.349 \times 10^4$	0.046 ± 0.0096
	12.3	13.679 ± 0.357	$-0.119 \pm 1.867 \times 10^{-2}$	$0.833 \pm 2.344 \times 10^{-2}$	0.374	$6.762 \times 10^5 \pm 2.983 \times 10^4$	0.0086 ± 0.0074
	8.8	7.643 ± 0.247	$-9.317 \times 10^{-2} \pm 2.101 \times 10^{-2}$	$0.769 \pm 2.184 \times 10^{-2}$	0.136	$4.357 \times 10^5 \pm 5.2641 \times 10^4$	0.0074 ± 0.068
	7.8	6.499 ± 0.130	$-8.229 \times 10^{-2} \pm 1.530 \times 10^{-2}$	$0.738 \pm 1.586 \times 10^{-2}$	0.057	$5.683 \times 10^5 \pm 2.783 \times 10^4$	0.0074 ± 0.0084
	6.3	5.961 ± 0.185	$3.077 \times 10^{-3} \pm 2.162 \times 10^{-2}$	$0.732 \pm 2.369 \times 10^{-2}$	0.097	$4.651 \times 10^5 \pm 5.236 \times 10^4$	0.0055 ± 0.0015
k^+	200	187.765 ± 0.926	$-2.151 \times 10^{-4} \pm 1.539 \times 10^{-2}$	$2.383 \pm 1.731 \times 10^{-2}$	6.996	$3.652 \times 10^5 \pm 3.873 \times 10^4$	0.173 ± 0.065
	62.4	222.355 ± 119.846	-0.926 ± 55.266	0.807 ± 51.701	33.128	$2.872 \times 10^5 \pm 4.652 \times 10^4$	0.074 ± 0.085
	17.3	31.241 ± 0.547	$1.127 \times 10^{-2} \pm 2.458 \times 10^{-2}$	$1.217 \pm 3.665 \times 10^{-2}$	1.736	$5.742 \times 10^5 \pm 3.836 \times 10^4$	0.073 ± 0.083
	12.3	25.626 ± 0.364	$-1.253 \times 10^{-3} \pm 1.743 \times 10^{-2}$	$1.093 \pm 2.373 \times 10^{-2}$	0.695	$5.951 \times 10^5 \pm 6.961 \times 10^4$	0.094 ± 0.0088
	8.8	21.825 ± 0.4389	$-2.923 \times 10^{-2} \pm 2.497 \times 10^{-2}$	$1.1218 \pm 2.821 \times 10^{-2}$	1.003	$6.847 \times 10^5 \pm 6.982 \times 10^4$	0.042 ± 0.0086
	7.8	21.775 ± 0.261	$1.206 \times 10^{-3} \pm 9.304 \times 10^{-3}$	$0.8289 \pm 1.197 \times 10^{-2}$	0.231	$7.092 \times 10^5 \pm 6.932 \times 10^4$	0.0073 ± 0.0017
	6.3	17.649 ± 0.407	$4.083 \times 10^{-2} \pm 1.434 \times 10^{-2}$	$0.665 \pm 1.475 \times 10^{-2}$	0.528	$6.942 \times 10^5 \pm 5.972 \times 10^4$	0.0072 ± 0.0062
$\bar{p}$	200	18.564 ± 0.432	$-2.735 \times 10^{-3} \pm 6.479 \times 10^{-2}$	$1.937 \pm 7.527 \times 10^{-2}$	1.131	$5.836 \times 10^5 \pm 6.917 \times 10^4$	0.941 ± 0.091
	62.4	11.551 ± 0.059	$-1.265 \times 10^{-4} \pm 1.416 \times 10^{-2}$	$1.326 \pm 1.149 \times 10^{-2}$	0.017	$3.803 \times 10^5 \pm 3.836 \times 10^4$	0.045 ± 0.0073
p	200	25.742 ± 0.539	$-8.487 \times 10^{-4} \pm 0.165$	3.617 ± 0.3166	2.433	$5.817 \times 10^5 \pm 6.5132 \times 10^4$	3.469 ± 0.947
	130	400.26 ± 0.285	0.984 ± 0.313	0.372 ± 0.03	34.071	$9.603 \times 10^5 \pm 5.271 \times 10^4$	7.872 ± 6.727
	62.4	24.232 ± 1.565	$-4.802 \times 10^{-2} \pm 14.652$	21.231 ± 16.460	16.75	$6.907 \times 10^5 \pm 7.826 \times 10^4$	22.116 ± 19.928

Table 3 The same as in Table 2 but for net-proton $p-\bar{p}$

Particle	$\sqrt{S_{NN}}$ (GeV)	c_0	c_1	c_2	c_3	χ^2/dof	V	m (GeV)
$p-\bar{p}$	17.3	12.853 ± 0.762	17.501 ± 0.0726	− 17.938 ± 0.064	− 140.123 ± 0.583	4.454	$6.482 \times 10^5 \pm 8.851 \times 10^4$	18.841 ± 62.871
	12.3	20.002 ± 2.420	− 1.913 ± 0.035	2.623 ± 0.053	18.509 ± 1.834	6.260	$5.719 \times 10^5 \pm 4.237 \times 10^4$	16.673 ± 48.821
	8.8	31.264 ± 0.579	− 1.786 ± 0.564	19.819 ± 1.876	17.579 ± 1.757	4.687	$3.451 \times 10^5 \pm 5.1492 \times 10^4$	0.793 ± 0.942
	7.8	32.135 ± 1.551	− 2.197 ± 0.254	37.869 ± 2.675	10.992 ± 1.565	3.156	$11.603 \times 10^5 \pm 7.605 \times 10^4$	0.076 ± 0.045
	6.3	44.269 ± 2.185	− 7.632 ± 0.754	6.814 ± 0.476	39.223 ± 2.869	7.367	$3.932 \times 10^5 \pm 4.139 \times 10^4$	0.0075 ± 0.0094

of the rapidity distributions of the various particles. The latter are likely isotropic and hence the overall results apparently match well with the Gaussian normal distribution. The corresponding parameters γ_2, $\bar{y}^n$, and σ_{m} can be related to the resulting fit parameters, $\gamma_2 = a_0$, $\bar{y}^n = a_1$, and $\sigma_{\mathrm{m}} = a_2$, Eq. (25).

The multiplicity per rapidity of the well-identified particles π^-, π^+, k^-, k^+, $\bar{p}$, p, and $p-\bar{p}$ measured in various high-energy experiments, at energies ranging from 6.3 to 5500 GeV, are successfully compared to the Cosmic Ray Monte Carlo (CRMC) event generator. The Carruthers and hadron resonance gas approaches are then fitted to both sets of results. We found that the Carruthers approach reproduces well the full range of multiplicity per rapidity for all produced particles, at the various energies, while the HRG approach fairly describes the results within a narrower rapidity range.

5. Conclusions

We have calculated the multiplicity per rapidity dN/dy for the well-identified hadrons π^-, π^+, k^-, k^+, $\bar{p}$, p, and $p-\bar{p}$ using two different approaches, namely HRG; a well-known framework based on thermal statistical assumptions and Carruthers approach based on correlations and fluctuations for hierarchy of the cumulant correlation functions and their linked-pair approximation, which in turn could be connected to negative binomial distributions and accordingly Gaussian- or exponential-like expressions for the rapidity distributions have been introduced.

The Carruthers and HRG approaches are then fitted to measurements at energies ranging from 6.3 to 5500 GeV and to corresponding simulations from the Cosmic Ray Monte Carlo (CRMC) event generator. The excellent agreement between the measurements and the simulations provides us with framework to compare between both approaches. We found that in the full range of rapidity, the multiplicity per rapidity is successfully reproduced in the Carruthers approach. The possible fluctuations and correlations as included in it seem to assure that the produced particles become isotropically distributed. On the other hand, the HRG approach restrictedly reproduces these anisotropic distributions. Accordingly, we conclude that the statistical assumptions alone—as included in the HRG approach—would not be able to apply on a wide range of rapidity. Ingredients assuring fluctuations and correlations including flow and interactions, if integrated in the HRG approach, would likely assure a better reproduction of the multiplicity per rapidity.

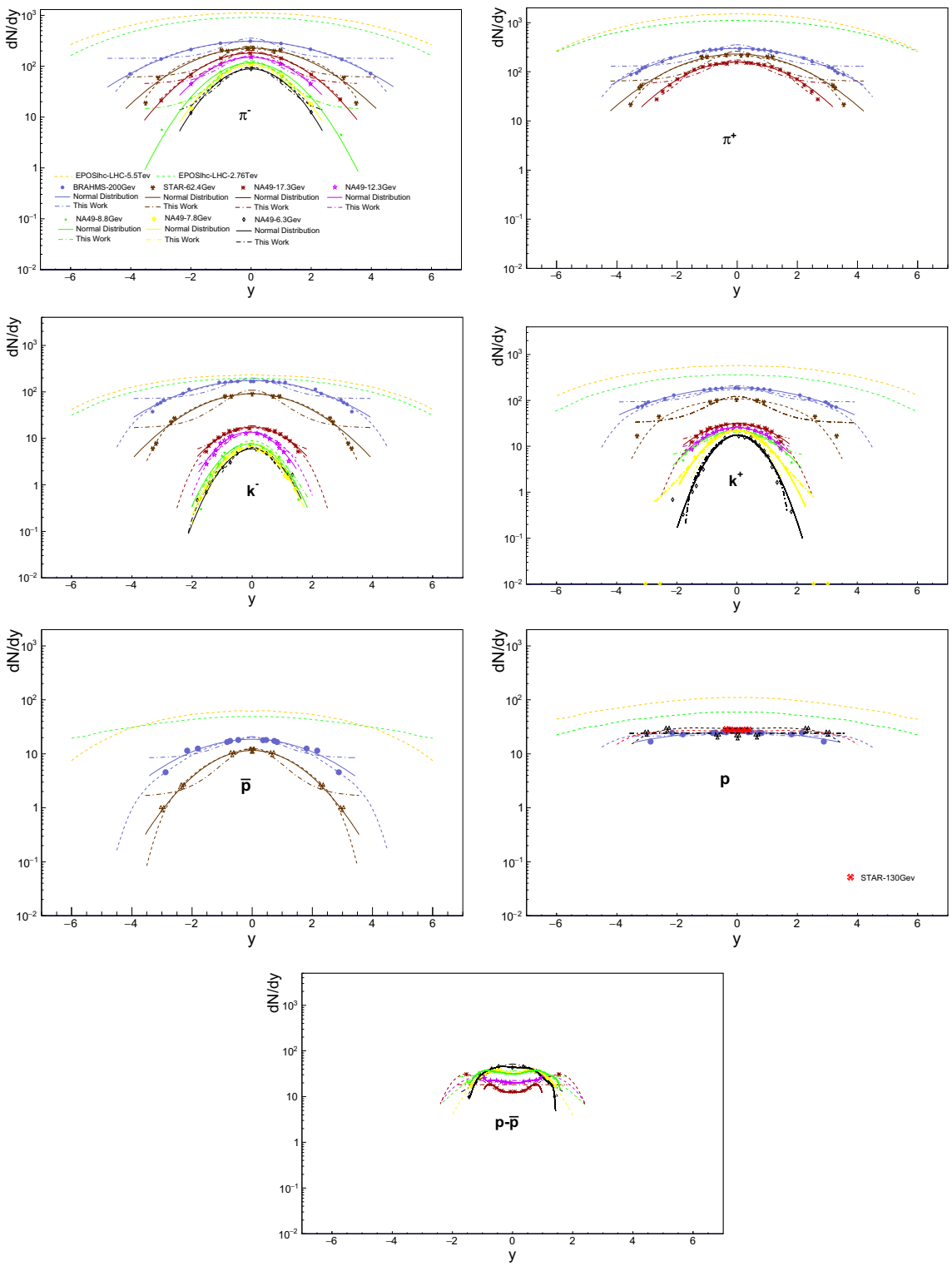

Fig. 1 (Color online) In semi-log scale, the multiplicity per rapidity for π^-, π^+, k^-, k^+, $\bar{p}$, p, and $p-\bar{p}$ particle yields is depicted as a function of the rapidity. The experimental results [34–36, 38–43] (symbols) are compared to the Cosmic Ray Monte Carlo (CRMC EPOSlhc) event generator (dashed curves), Sect. 3, and also fitted to the hadron resonance gas (HRG) approach (dash-dotted curves), Eq. (6) or Eq. (25) and to the Gaussian distribution function (solid curve)

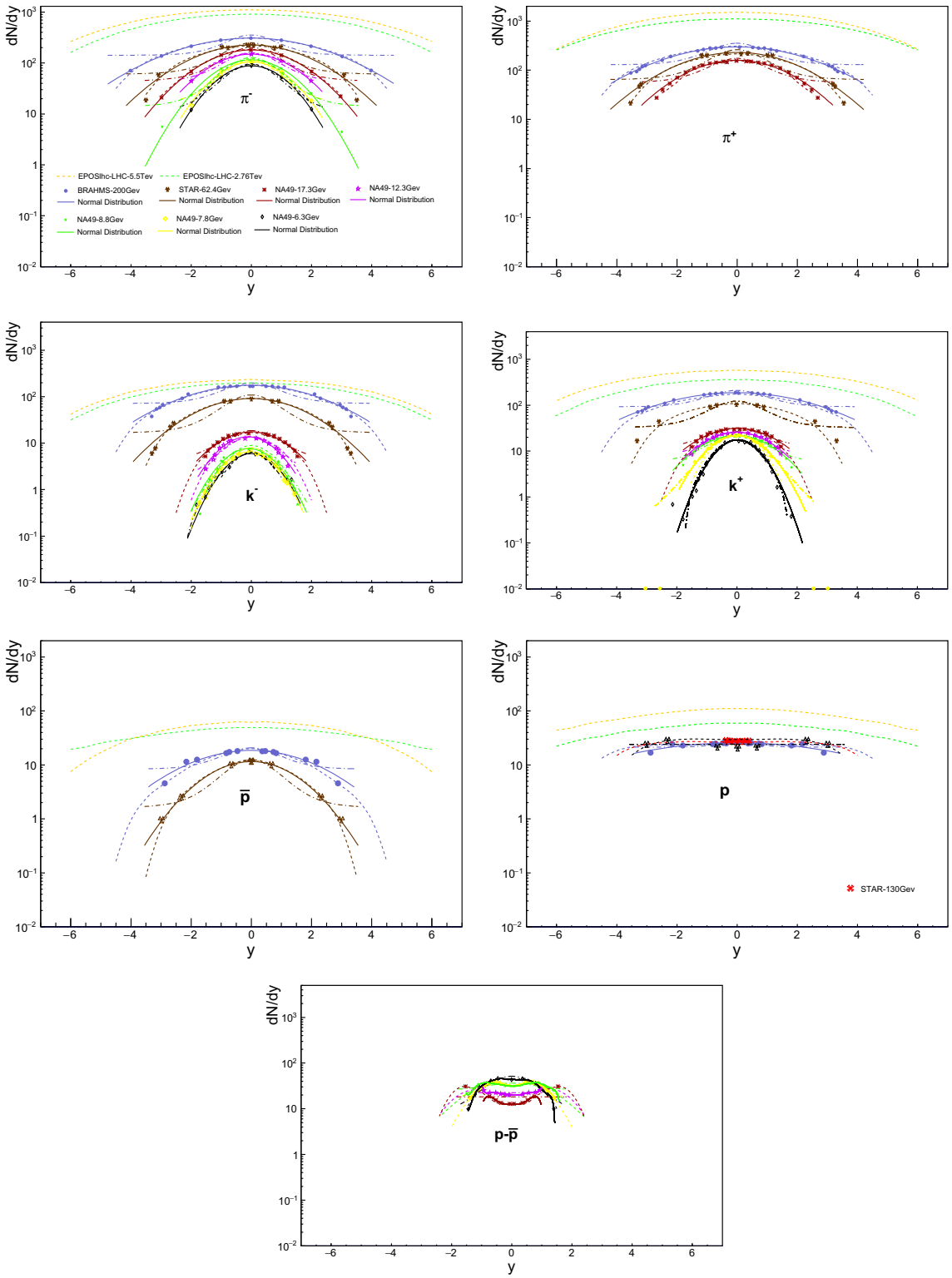

Fig. 2 The same as in Fig. 1 but here for Carruthers rapidity approach

Appendix: Mathematical details for Eq. (6)

The Grand canonical partition function reads

$$Z(T,V,\mu) = \ \mathrm{Tr}\left[\exp\left(\frac{\mu N - H}{\mathrm{T}}\right)\right], \tag{27}$$

where H is Hamiltonian of the system, N is the total number of constituents. In the HRG model, Eq. (27) can be expressed as a sum over all hadron resonances as

$$\begin{aligned}\ln Z(T,V,\mu) &= \sum_i \ln Z_i(T,V,\mu) \\ &= \frac{Vg_i}{(2\pi)^3}\int_0^\infty \pm d^3p \ln\left[1 \pm \exp\left(\frac{\varepsilon_i(p)-\mu_i}{\mathrm{T}}\right)\right],\end{aligned} \tag{28}$$

where $\pm$ stands for bosons and fermions, respectively, and $\varepsilon_i = \left(p^2 + m_i^2\right)^{1/2}$ is the dispersion relation of the ith particle. The total number of particles can be obtained from the partition function as follows.

$$\begin{aligned}N_i &= T\frac{\partial Z_i(T,V)}{\partial \mu_i} \\ &= \frac{Vg_i}{(2\pi)^3}\int_0^\infty d^3p\left[\exp\left(\frac{\varepsilon_i(p)-\mu_i}{\mathrm{T}}\right) \pm 1\right]^{-1},\end{aligned} \tag{29}$$

The invariant momentum spectrum of partially radiated by a thermal source is given by

$$\frac{\mathrm{d}^3N_i}{\mathrm{d}y m_T \mathrm{d}m_T \mathrm{d}\phi} = \varepsilon_i \frac{Vg_i}{(2\pi)^3}\left[\exp\left(\frac{\varepsilon_i(p)-\mu_i}{\mathrm{T}}\right) \pm 1\right]^{-1}, \tag{30}$$

where m_T is the transverse mass. This is given by

$$m_T = \sqrt{m^2 + p_T^2}, \tag{31}$$

where p_T is the transverse momentum. The energy of the ith particle ε_i can be expressed in terms of the rapidity (y) and m_T

$$\varepsilon = m_T \cosh(y). \tag{32}$$

Then, the rapidity density can be obtained through integral over the full transverse mass m_T,

$$\begin{aligned}\frac{\mathrm{d}N}{\mathrm{d}y} &= \frac{Vg_i}{(2\pi)^2}\int_m^\infty dm_\mathrm{T}\cosh(y)m_\mathrm{T}^2 \\ &\left[\exp\left(\frac{m_\mathrm{T}\cosh(y)-\mu_i}{T}\right) \pm 1\right]^{-1}.\end{aligned} \tag{33}$$

To make the lower integration limit starts from zero, we define a new variable t

$$t = \frac{m_T - m}{T}\cosh(y), \tag{34}$$

Equation (34) can be arranged as

$$m_T = \frac{tT}{\cosh(y)} + m, \tag{35}$$

By differentiating Eq. (35), we get

$$dm_T = \frac{Tdt}{\cosh(y)}, \tag{36}$$

By substituting Eqs. (34), (35) and (36) into Eq. (33), we get

$$\frac{\mathrm{d}N}{\mathrm{d}y} = \frac{Vg_i}{(2\pi)^2}\int_0^\infty \frac{\cosh(y)(\frac{tT}{\cosh(y)} + m)^2 T\mathrm{d}t}{\cosh(y)\left[\exp(t + \frac{m}{T}\cosh(y) - \frac{\mu_i}{T}) \pm 1\right]}, \tag{37}$$

Also, Eq. (37) can be rewritten as

$$\frac{\mathrm{d}N}{\mathrm{d}y} = \frac{Vg_iT^3}{(2\pi)^2\cosh^2(y)}\int_0^\infty \frac{(t + \frac{m\cosh(y)}{T})^2\mathrm{d}t}{\left[\exp(t + \frac{m}{T}\cosh(y) - \frac{\mu_i}{T}) \pm 1\right]}. \tag{38}$$

Let us define

$$c = \frac{m\cosh(y) - \mu_i}{T}. \tag{39}$$

Then, Eq. (38) can be rewritten as

$$\frac{\mathrm{d}N}{\mathrm{d}y} = \frac{Vg_iT^3}{(2\pi)^2\cosh^2(y)}\int_0^\infty \frac{(t^2 + \frac{2m\cosh(y)t}{T} + \frac{m^2\cosh^2(y)}{T^2})dt}{\exp(t+c) \pm 1}, \tag{40}$$

Also, Eq. (40) can be rewritten as

$$\begin{aligned}\frac{\mathrm{d}N}{\mathrm{d}y} &= \frac{Vg_iT^3}{(2\pi)^2\cosh^2(y)} \\ &\left\{\int_0^\infty \frac{t^2\mathrm{d}t}{\exp(t+c)\pm 1} + \frac{2m\cosh(y)}{T}\int_0^\infty \frac{t\mathrm{d}t}{\exp(t+c)\pm 1}\right. \\ &\left. + \frac{m^2\cosh(y)}{T^2}\int_0^\infty \frac{\mathrm{d}t}{\exp(t+c)\pm 1}\right\}.\end{aligned} \tag{41}$$

The polylogarithmic function is defined as

$$\mp L_i s(\mp z) = \frac{1}{\Gamma(s)}\int_0^\infty \frac{t^{s-1}dt}{\frac{\exp(t)}{z} \pm 1}, \tag{42}$$

where

$$\begin{aligned}L_{i1}(z) &= \log(1+z) \\ \Gamma(s) &= (s-1)!, \\ L_{in}(z) &= \sum_k = 1^\infty \frac{z^k}{k^n}.\end{aligned} \tag{43}$$

By substituting from Eqs. (39), (42) and (43) into Eq. (41), we get

$$\frac{dN}{dy} = \frac{g_i V}{2\pi^2}\left\{\frac{2T^3 L_{i3}}{\cosh^2(y)}(\mp\exp(-c)) \mp \frac{2mT^2}{\cosh(y)}L_{i2}(\mp\exp(-c)). \pm m^2 T\log(1\pm(\mp\exp(-c)))\right\}. \quad (44)$$

By substituting Eq. (39) into Eq. (44), the multiplicity per rapidity reads

$$\frac{dN}{dy} = \frac{g_i V}{2\pi^2}\left\{\frac{2T^3 L_{i3}}{\cosh^2(y)}\left[\mp\exp\left(-\frac{m\cosh(y)-\mu_i}{T}\right)\right] \mp \frac{2mT^2}{\cosh(y)}L_{i2}\left[\mp\exp\left(-\frac{m\cosh(y)-\mu_i}{T}\right)\right] \pm m^2 T\log\left(1\pm\left[\mp\exp\left(-\frac{m\cosh(y)-\mu_i}{T}\right)\right]\right)\right\}. \quad (45)$$

Acknowledgements The work of AT was supported by the ExtreMe Matter Institute (EMMI) at the GSI Helmholtz Centre for Heavy Ion Research, Visiting Professor 2019.

References

[1] A N Tawfik *Int. J. Mod. Phys.* **A29** 1430021 (2014)
[2] H Satz *Rept. Prog. Phys.* **63** 1511 (2000)
[3] B Muller *Rep. Prog. Phys.* **58** 611 (1995)
[4] E V Shuryak *Phys. Rep.* **61** 71 (1980)
[5] J Cleymans, K Redlich, H Satz and E Suhonen *Z. Phys.* **C33** 151 (1986)
[6] J Cleymans and H Satz *Z. Phys.* **C57** 135 (1993)
[7] H Kouno and F Takagi *Z. Phys.* **C42** 209 (1989)
[8] A Andronic, P Braun-Munzinger, J Stachel and M Winn *Phys. Lett.* **B718** 80 (2012)
[9] S K Tiwari, P K Srivastava and C P Singh *J. Phys.* **G40** 045102 (2013)
[10] P K Srivastava and C P Singh *Phys. Rev.* **D85** 114016 (2012)
[11] R Hagedorn and J Rafelski *Phys. Lett.* **97B** 136 (1980)
[12] L Marques, J Cleymans and A Deppman *Phys. Rev.* **D91** 054025 (2015)
[13] S K Tiwari, P K Srivastava and C P Singh *Phys. Rev.* **C85** 014908 (2012)
[14] J D Bjorken *Phys. Rev.* **D27** 140 (1983)
[15] E Schnedermann and U W Heinz *Phys. Rev. Lett.* **69** 2908 (1992)
[16] E Schnedermann, J Sollfrank and U W Heinz *Phys. Rev.* **C48** 2462 (1993)
[17] P Braun-Munzinger, J Stachel, J P Wessels and N Xu *Phys. Lett.* **B365** 1 (1996)
[18] P Braun-Munzinger, J Stachel, J P Wessels and N Xu *Phys. Lett.* **B344** 43 (1995)
[19] S Q Feng and Y Zhong *Phys. Rev.* **C83** 034908 (2011)
[20] S Feng and X Yuan *Sci. China* **G52** 198 (2009)
[21] S Uddin, J S Ahmad, W Bashir and R A Bhat *J. Phys.* **G39** 015012 (2012)
[22] T Hirano, K Morita, S Muroya and C Nonaka *Phys. Rev.* **C65** 061902 (2002)
[23] K Morita, S Muroya, C Nonaka and T Hirano *Phys. Rev.* **C66** 054904 (2002)
[24] J Manninen, E L Bratkovskaya, W Cassing and O Linnyk *Eur. Phys. J.* **C71** 1615 (2011)
[25] U Mayer and U W Heinz *Phys. Rev.* **C56** 439 (1997)
[26] W Broniowski and W Florkowski *Phys. Rev. Lett.* **87** 272302 (2001)
[27] W Broniowski and W Florkowski *Phys. Rev.* **C65** 064905 (2002)
[28] P Bozek *Phys. Rev.* **C77** 034911 (2008)
[29] A N Tawfik, M A Wahab, H Yassin and H M N El Din *J. Exp. Theor. Phys.* **130** 506 (2020)
[30] H Yassin, E R A Elyazeed and A N Tawfik arXiv:2003.02675 [hep-ph]
[31] A N Tawfik, M A Wahab, H Yassin and H N El Din *J. Exp. Theor. Phys.* **157** 604 (2020)
[32] F Becattini and J Cleymans *J. Phys.* **G34** S959 (2007)
[33] J Cleymans, J Strumpfer and L Turko *Phys. Rev.* **C78** 017901 (2008)
[34] J H Lee et al BRAHMS (Collaboration) *J. Phys.* **G30** S85 (2004)
[35] S V Afanasiev et al (The NA49 Collaboration) *Phys. Rev.* **C66** 054902 (2002)
[36] I G Bearden et al (NA44 Collaboration) *Phys. Rev.* **C66** 044907 (2002)
[37] B Biedron and W Broniowski *Phys. Rev.* **C75** 054905 (2007)
[38] E L Bratkovskaya, A Palmese, W Cassing, E Seifert, T Steinert and P Moreau *J. Phys. Conf. Ser.* **878** 012018 (2017)
[39] J Adams et al (STAR Collaboration) *Phys. Rev.* **C70** 041901 (2004)
[40] W P Zhou, S H Cai and Z W Long *Chin. Phys.* **C33** 10 (2009)
[41] K Hebeler, S K Bogner, R J Furnstahl, A Nogga and A Schwenk . **C83** 031301 (2011)
[42] I G Bearden et al (BRAHMS Collaboration) *Phys. Rev. Lett.* **94** 162301 (2005)
[43] P Seyboth et al (NA49 Collaboration) *Acta Phys. Polon.* **B36** 565 (2005)
[44] C Adler et al (STAR Collaboration) *Phys. Rev. Lett.* **87** 262302 (2001)
[45] K Adcox et al (PHENIX Collaboration) *Phys. Rev.* **C69** 024904 (2004)
[46] N N Kalmykov, S S Ostapchenko and A I Pavlov *Nucl. Phys. Proc. Suppl.* **52** 17 (1997)
[47] N N Kalmykov and S S Ostapchenko *Phys. Atom. Nucl.* **56** 346 (1993) [*Yad. Fiz.* 56 no **3** 105 (1993)]
[48] S Ostapchenko *Phys. Rev.* **D74** 014026 (2006)
[49] S Ostapchenko *Nucl. Phys. Proc. Suppl.* **151** 143 (2006)
[50] S Ostapchenko *AIP Conf. Proc.* **928** 118 (2007)
[51] J Engel, T K Gaisser, T Stanev and P Lipari *Phys. Rev.* **D46** 5013 (1992)
[52] R S Fletcher, T K Gaisser, P Lipari and T Stanev *Phys. Rev.* **D50** 5710 (1994)
[53] E J Ahn, R Engel, T K Gaisser, P Lipari and T Stanev *Phys. Rev.* **D80** 094003 (2009)
[54] K Werner, F M Liu and T Pierog *Phys. Rev.* **C74** 044902 (2006)
[55] T Pierog and K Werner *Nucl. Phys. Proc. Suppl.* **196** 102 (2009)
[56] M Tanabashi et al (Particle Data Group) *Phys. Rev.* **D98** 030001 (2018)
[57] S Capstick and N Isgur *Phys. Rev.* **D34** 2809 (1986) [*AIP Conf. Proc.* **132** 267(1985)]
[58] A N Tawfik, H Yassin and E R A Elyazeed (2019) arXiv:2003.02675 [hep-ph]
[59] A N Tawfik *Adv. High Energy Phys.* **2019** 4604608 (2019)

[60] A N Tawfik and E Abbas *Phys. Part. Nucl. Lett.* **12** 521 (2015)
[61] P. Carruthers *Proceedings of the XIII Warsaw symposium on Elementary Particle Physics* p 317 (1990)
[62] P Carruthers, H C Eggers, Q Gao and I Sarcevic *Int. J. Mod. Phys.* **A6** 3031 (1991)
[63] J Randrup *Acta Phys. Hung.* **A22** 69 (2005)
[64] T Pierog, I Karpenko, J M Katzy, E Yatsenko and K Werner *Phys. Rev.* **C92** 034906 (2015)
[65] A Bazavov et al *Phys. Rev. Lett.* **113** 072001 (2014)
[66] P ManLo, M Marczenko, K Redlich and C Sasaki *Eur. Phys. J.* **A52** 235 (2016)